Title Page

Monitoring Tumor Response to Linifanib Therapy with SPECT/CT Using the Integrin $\alpha_v\beta_3$-Targeted Radiotracer ^{99m}Tc-3P-RGD$_2$

Shundong Ji, Yang Zhou, Martin J. Voorbach, Guoqiang Shao, Yumin Zhang, Gerard B. Fox, Daniel H. Albert, Yanping Luo, Shuang Liu, Sarah R. Mudd

School of Health Sciences, Purdue University, IN 47907, USA: SJ, Y Zhou, GS, SL

AbbVie Inc., Translational Sciences, Dept. R4DF, Bldg. AP4, 1 North Waukegan Road, North Chicago, IL 60064: MJV, Y Zhang, GBF, YL, SRM

AbbVie Inc., *In Vivo* Pharmacology, Dept. R4N2, Bldg. AP3-1, 1 North Waukegan Road, North Chicago, IL 60064: DHA

RUNNING TITLE Page

^{99m}Tc-3P-RGD$_2$: an $\alpha_v\beta_3$ tracer to monitor Linifanib therapy

*****Correspondence should be addressed: Dr. Shuang Liu, the School of Health Sciences, Purdue University, 550 Stadium Mall Drive, West Lafayette, IN 47907; Email: lius@pharmacy.purdue.edu

28 Pages

6 Figures

48 References

Abstract: 240 words

Introduction: 687 words

Discussion: 811 words

Abbreviations:

SPECT, single photon emission computed tomography; CT, computed tomography; H&E, hematoxylin and eosin; IHC, immunohistochemistry; DCE-MRI, dynamic contrast enhanced magnetic resonance imaging; PET, positron emission tomography; VEGFR, vascular endothelial growth factor receptor; PDFGR, platelet-derived growth factor receptor; %ID/cm^3, percent injected dose per centimeter cubed; TKi, tyrosine kinase inhibitor; T/M, tumor to muscle; NSCLC, non-small cell lung cancer; POSEM, pixelated ordered subsets by expectation maximization; FITC, fluorescein isothiocyanate; FWHM, full-width half-maximum; ROI, region of interest; ANOVA, analysis of variance; PD, pharmacodynamic; ECM, extracellular matrix;

Section: Drug Discovery and Translational Medicine

JPET Fast Forward. Published on June 7, 2013 as DOI: 10.1124/jpet.112.202622
This article has not been copyedited and formatted. The final version may differ from this version.

ABSTRACT

The objective of this study was to determine the utility of ^{99m}Tc-3P-RGD$_2$ SPECT/CT for noninvasive monitoring of integrin $\alpha_v\beta_3$ expression response to antiangiogenic treatment with linifanib. Linifanib or vehicle therapy was carried out in female athymic *nu/nu* mice bearing U87MG glioma (high $\alpha_v\beta_3$ expression) or PC-3 prostate (low $\alpha_v\beta_3$ expression) tumors at 12.5 mg/kg twice daily. The average tumor volume was 180 ± 90 mm^3 the day prior to baseline SPECT/CT. Longitudinal ^{99m}Tc-3P-RGD$_2$ SPECT/CT imaging was performed at baseline (-1 day) and days, 1, 4, 11, and 18. Tumors were harvested at all imaging time points for histopathological analysis with hematoxylin and eosin (H&E) and IHC. A significant difference in tumor volumes between vehicle- and linifanib- treated groups was observed after 4 days of linifanib therapy in the U87MG model. The %ID tumor uptake of ^{99m}Tc-3P-RGD$_2$ peaked in the vehicle-treated group at day 11, while the %ID/cm^3 tumor uptake decreased slowly over the whole study period. During the first 2 days of linifanib treatment, a rapid decrease in both %ID/cm^3 tumor uptake and tumor / muscle ratios of ^{99m}Tc-3P-RGD$_2$ was observed, followed by a slow decrease until day 18. No decrease in tumor uptake of ^{99m}Tc-3P-RGD$_2$ or tumor volume was observed for either treatment group in the PC-3 model. Changes in tumor vasculature were confirmed by histopathological H&E analysis and IHC. Longitudinal imaging using ^{99m}Tc-3P-RGD$_2$ SPECT/CT may be a useful tool for monitoring the downstream biological effects of linifanib therapy.

JPET Fast Forward. Published on June 7, 2013 as DOI: 10.1124/jpet.112.202622
This article has not been copyedited and formatted. The final version may differ from this version.

INTRODUCTION

Inhibiting angiogenesis is a promising strategy for cancer therapy (Dunn et al., 2000; Bergers and Benjamin, 2003; Bergers et al., 2003; Ferrara and Kerbel, 2005). As antiangiogenic therapies have become more common, finding suitable translational biomarkers for antiangiogenic modulation of the tumor vasculature has become more important (Cao et al., 2011). Microvessel density has been proposed as a prognostic indicator of progression, overall survival, and disease-free survival in cancer patients. Evaluation of microvessel density is typically performed by immunostaining endothelial cells in tumor tissues and counting the number of vessels using a high power field microscope. This approach is not practical for routine monitoring of antiangiogenic therapy due to the invasive nature of the procedure. DCE-MRI has been used to measure perfusion properties of tumors, but this method can be technically challenging and standardization is complex (Jeswani and Padhani, 2005; O'Connor et al., 2007). PET and SPECT tracers have been developed to evaluate expression of certain integrins, particularly $\alpha_v\beta_3$, which are involved in angiogenesis. The need for a cyclotron and lack of simple kit preparation presents a significant challenge for current ^{18}F-labeled radiotracers for more routine imaging of integrin expression. Therefore, there is an unmet need for radiotracers that are readily available and clinically useful for early detection of integrin $\alpha_v\beta_3$-positive tumors and metastases and for monitoring antiangiogenic therapy.

Integrins are receptors involved in cell adhesion and migration of endothelial cells (Desgrosellier and Cheresh, 2010). It is known that the cross-talk between receptor tyrosine kinases and integrin receptors is crucial for many cellular functions. Interactions between $\alpha_v\beta_3$ and VEGFR2/PDGFR seem to be particularly important for vascularization (Cybulsky et al., 1994; Jones et al., 1997; Heldin et al., 1998; Woodard et al., 1998; Clemmons et al., 1999; Soldi et al., 1999; Borges et al., 2000; Mahabeleshwar et al., 2007; Somanath et al., 2009). This relationship regulates many cellular activities during angiogenesis, including endothelial cell

JPET Fast Forward. Published on June 7, 2013 as DOI: 10.1124/jpet.112.202622
This article has not been copyedited and formatted. The final version may differ from this version.

migration, survival and tube formation, and hematopoietic cell functions within the vasculature (Somanath et al., 2009; Desgrosellier and Cheresh, 2010). Thus, monitoring $\alpha_v\beta_3$ expression is of interest for antiangiogenic therapies.

Many extracellular matrix proteins interact with $\alpha_v\beta_3$ via the Arg-Gly-Asp (RGD) tripeptide sequence. Over the last several years, there has been interest in radiolabeled multimeric cyclic RGD peptides as radiotracers for tumor imaging by SPECT or PET (Shi et al., 2009a; Shi et al., 2009b; Chakraborty et al., 2010; Shi et al., 2011; Zhou et al., 2012a). ^{99m}Tc-3P-RGD$_2$ is a ^{99m}Tc-labeled cyclic RGD peptide dimer. It is readily prepared from $^{99m}TcO_4^-$ with high specific activity using a kit formulation, making it easily accessible (Wang et al., 2009; Jia et al., 2011). In several preclinical models, ^{99m}Tc-3P-RGD$_2$ showed high tumor uptake, rapid renal clearance, and high metabolic stability (Wang et al., 2009; Jia et al., 2011; Zhou et al., 2011). ^{99m}Tc-3P-RGD$_2$ tumor uptake measured by %ID/cm^3 and T/M ratio had a linear correlation with tumor β_3 and CD31, a marker for tumor blood vessels, expression levels (Zhou et al., 2011; Zhou et al., 2012a). ^{99m}Tc-3P-RGD$_2$ SPECT/CT was also used for accurate quantification of tumor radioactivity accumulation and delineation of tumor necrotic regions (Zhou et al., 2012b; Shao et al., 2013). It is currently under clinical investigation as a new SPECT radiotracer for imaging carcinomas of breast and lung in cancer patients (Ma et al., 2011; Zhu et al., 2012).

Linifanib (ABT-869) is a multi-targeted receptor tyrosine kinase inhibitor (TKi), specifically targeting VEGF and PDGF receptors (Albert et al., 2006; Zhou et al., 2009; Jiang et al., 2011). *In vitro,* linifanib was shown to inhibit the phosphorylation of members of the VEGF and PDGF receptor families (Shankar et al., 2007; Hernandez-Davies et al., 2011). Treatment with Linifanib resulted in pronounced regression of tumors *in vivo* in a variety of pre-clinical tumor models (Albert et al., 2006). Phase II studies showed promising results in breast cancer, metastatic NSCLC, and liver cancer (Tannir et al., 2011). Here we determined the utility of imaging ^{99m}Tc-3P-RGD$_2$ tumor uptake as a biomarker for antiangiogenic treatment with linifanib

JPET Fast Forward. Published on June 7, 2013 as DOI: 10.1124/jpet.112.202622
This article has not been copyedited and formatted. The final version may differ from this version.

in the U87MG glioma xenograft model, which has a high vessel density and $\alpha_v\beta_3$ expression, and the PC-3 prostate cancer model, which has low vessel density and $\alpha_v\beta_3$ expression.

JPET Fast Forward. Published on June 7, 2013 as DOI: 10.1124/jpet.112.202622
This article has not been copyedited and formatted. The final version may differ from this version.

METHODS

Chemicals and Analytical Method. Trisodium triphenylphosphine-3,3',3''-trisulfonate (TPPTS) and tricine were purchased from *Sigma/Aldrich* and were used without further purification. HYNIC-3P-RGD_2 (HYNIC = 6-(2-(2-sulfonatobenzaldehyde)hydrazono)nicotinyl; 3P-RGD_2 = PEG_4-E[PEG_4-c(RGDfK)]$_2$, and PEG_4 = 15-amino-4,7,10,13-tetraoxapentadecanoic acid) were prepared according to previously reported methods (Wang et al., 2009; Jia et al., 2011). $Na^{99m}TcO_4$ was obtained from Cardinal HealthCare (Chicago, IL). The radio-HPLC method used a LabAlliance system equipped with a β-ram IN-US detector and Zorbax C_{18} column (4.6 mm x 250 mm, 300 Å pore size) with a flow rate of 1 mL/min. The mobile phase was isocratic with 90% solvent A (25 mM NH_4OAc buffer, pH = 5.0) and 10% solvent B (acetonitrile) at 0 – 5 min, followed by a gradient mobile phase from 10% B at 5 min to 40% B at 20 min.

^{99m}Tc-3P-RGD_2 Synthesis and Dose Preparation. ^{99m}Tc-3P-RGD_2 was prepared according to a previously published method (Wang et al., 2009; Jia et al., 2011) using a lyophilized kit formulation prepared in-house, which contains 20 μg HYNIC-3P-RGD_2, 5 mg TPPTS, 6.5 mg tricine, 40 mg mannitol, 38.5 mg disodium succinate hexahydrate and 12.7 mg succinic acid. ^{99m}Tc-labeling was accomplished by adding 1 – 1.5 mL of $Na^{99m}TcO_4$ solution (1,110 – 1,850 MBq) to the HYNIC-3P-RGD_2 mixture. The reconstituted vial was then heated at 100 °C for 30 min. The resulting solution was analyzed by radio-HPLC. The radiochemical purity was >90%. Doses were prepared by dissolving the radiotracer in saline to a concentration of 370 – 525 MBq/mL for imaging studies.

Animal Models. The animal protocol was reviewed and approved by the Purdue University Animal Care and Use Committee and by the AbbVie Institutional Animal Care and Use Committee. All studies were conducted in Association for Assessment and Accreditation of Laboratory Animal Care accredited facilities. U87MG and PC-3 cell lines were obtained from

JPET Fast Forward. Published on June 7, 2013 as DOI: 10.1124/jpet.112.202622
This article has not been copyedited and formatted. The final version may differ from this version.

American Type Culture Collection (Manassas, VA). U87MG cells were cultured in the Minimum Essential Medium while PC-3 cells were cultured in the F-12 medium (GIBCO, Grand Island, NY). All cells were supplemented with 10% fetal bovine serum (ATCC, Manassas, VA) and 1% penicillin and streptomycin solution (GIBCO Industries Inc., Langley, OK) at 37 °C in a humidified atmosphere of 5% CO_2 in air. Cells were grown as a monolayer and were harvested or split when they reached 90% confluence to maintain exponential growth. Female athymic *nu/nu* mice were purchased from Harlan (Indianapolis, IN) at 4 – 5 weeks of age. Each mouse was implanted subcutaneously near the shoulder with 5×10^6 cells. The tumor volume was measured every two days for the first two weeks, and every day for next 3 weeks with digital calipers. The tumor volume was calculated using the formula: $Tumor\ Volume = \frac{Length \times Width^2}{2}$.

Treatment Protocol. Groups (n = 8 – 10) were size-matched with an average tumor volume of 180 ± 90 mm^3 one day before baseline SPECT/CT imaging. This occurred three weeks after inoculation for U87MG tumors and 4 weeks after PC-3 inoculation. Vehicle (0.15% hydroxypropylmethyl cellulose, 2% ethanol, 5% Tween 80, 20% PEG400, 73% saline) or linifanib treatment was initiated at a dose of 12.5 mg/kg on day 0 after baseline imaging. Linifanib (Abbott Laboratories, Abbott Park, IL) was dosed orally twice daily, with a time interval of >8 h between consecutive doses.

Imaging Protocol for SPECT/CT. Longitudinal SPECT/CT imaging was performed at baseline (-1), 1, 4, 11, and 18 days after treatment initiation using a micro-SPECT-II/CT scanner (Milabs, Utrecht, The Netherlands) equipped with 0.6 mm multi-pinhole collimators. One hour prior to SPECT/CT imaging, 37 – 55.5 MBq ^{99m}Tc-3P-RGD_2 in 0.1 – 0.2 mL of saline was administered intravenously via the lateral tail vein. Linifanib was dosed approximately two hours prior to SPECT/CT imaging. Anesthesia was induced using an air flow rate of 350 mL/min and approximately 3.0% isoflurane. After induction of anesthesia, the air flow rate was reduced to 250 mL/min with approximately 2.0% isoflurane. Animals were maintained at 37°C during

JPET Fast Forward. Published on June 7, 2013 as DOI: 10.1124/jpet.112.202622
This article has not been copyedited and formatted. The final version may differ from this version.

image acquisition. SPECT images were acquired using 75 projections over 30 minutes. After SPECT acquisition, CT imaging was performed using 'normal' acquisition settings (2 degree intervals) at 45 kV and 500 μA.

Image Reconstruction and Data Processing. SPECT images were reconstructed using a POSEM (pixelated ordered subsets by expectation maximization) algorithm with 6 iterations and 16 subsets. CT data was reconstructed using a cone-beam filtered back-projection algorithm (NRecon v1.6.3, Skyscan). After reconstruction, the SPECT and CT data were automatically co-registered and re-sampled to equivalent voxel sizes. Co-registered images were further rendered and visualized using PMOD software (PMOD Technologies, Zurich, Switzerland). A 3D-Guassian filter (0.8 mm FWHM) was applied to smooth noise and the look up tables were adjusted for good visual contrast. Reconstructed images were visualized as both orthogonal slices and maximum intensity projections. All images presented are normalized for injected dose for visual comparison.

Radioactivity Quantification. Radiation sources of known radioactivity were imaged and reconstructed using the same scanning protocol described above. A standard curve was generated to correlate the pixel intensities in the reconstructed images to the radioactivity as measured by a γ-counter. The ROIs were drawn manually to cover the entire tumor based on transverse view of the CT image. For tumor delineation with SPECT, a threshold of 50% or more of the maximum pixel value on the SPECT image was chosen. Tumor volume and radioactivity counts were generated by using the PMOD software (PMOD Technologies, Zurich, Switzerland) and the amount of radioactivity in each tumor was calculated according to the above mentioned standard curve. Tumor uptake of ^{99m}Tc-3P-RGD$_2$ was expressed as %ID and %ID/cm^3. Reference ROIs were drawn over muscle as background radioactivity for T/M ratio calculations.

JPET Fast Forward. Published on June 7, 2013 as DOI: 10.1124/jpet.112.202622
This article has not been copyedited and formatted. The final version may differ from this version.

Protocol for Tumor Immunostaining. Tumors were cut into two pieces for immunostaining and H&E staining (n = 3 – 5 tumors per time point). After harvesting tumors, the tumors sections for immunostaining were immediately snap-frozen in optical cutting temperature solution (Sakara, Torrance, CA). Tumors were then cut into 5 μm slices. After thorough drying at room temperature, slides were fixed with ice-cold acetone for 10 min, and air dried for 20 min at room temperature. The sections were blocked with 10% goat serum (Jackson ImmunoResearch Inc., West Grove, PA) for 30 min at room temperature and then incubated with hamster anti-integrin β_3 antibody (1:100, BD Biosciences, San Jose, CA) and rat anti-CD31 antibody (1:100, BD Biosciences, San Jose, CA) for 1 h at room temperature. A β_3 antibody was chosen to represent $\alpha_v\beta_3$ because the only other integrin with a β_3 subunit besides $\alpha_v\beta_3$ is expressed on platelets. The majority of β_3 in the tumor sections is likely to be on the vasculature and tumor cells (Shattil, 1995). After incubating with Cy3-conjugated goat anti-hamster (1:100, Jackson ImmunoResearch Inc., West Grove, PA) and FITC-conjugated goat anti-rat secondary antibodies (1:100, Jackson ImmunoResearch Inc., West Grove, PA) the sections were washed with PBS. Fluorescence was visualized with a Nikon fluorescence microscope (Nikon Instruments, Melville, NY).

Histopathological H&E Staining. Histopathological analysis was performed by hematoxylin and eosin (H&E) staining of tumors according to previously published methods (Zhou et al., 2011). Briefly, all the tissues were fixed in 10% neutral buffered formalin. Tissues were embedded in paraffin and 4 μm sections were de-paraffinized and rehydrated through graded alcohols. Sections were stained for H&E to evaluate the morphology and then examined under light microscope. Aperio's ImageScope Viewer (Vista, CA) was used to visualize the whole-slide digital scans and capture images.

Statistical Analysis. All data were expressed as the mean plus or minus the standard error of the mean. Statistical analyses were performed by two-way ANOVA followed by the

Newman-Keuls test for multiple comparisons to compare treatment groups. The level of significance was set at $p < 0.05$. A one-way ANOVA was performed to determine changes over time. GraphPad Prism 5 (GraphPad Software Inc., La Jolla, CA) was used for linear and nonlinear regression analysis.

JPET Fast Forward. Published on June 7, 2013 as DOI: 10.1124/jpet.112.202622
This article has not been copyedited and formatted. The final version may differ from this version.

RESULTS

In this study, ^{99m}Tc-3P-RGD$_2$ SPECT/CT was used to monitor linifanib therapy in the xenografted U87MG glioma and PC-3 prostate cancer models. ^{99m}Tc-3P-RGD$_2$ was prepared in high yield and radiochemical purity (RCP >90%) with high specific activity (> 185 MBq/μg or 370 GBq/μmol). Linifanib and ^{99m}Tc-3P-RGD$_2$ were well tolerated in all studies.

Linifanib Therapy in the U87MG Model. Figure 1A compares the tumor volumes for both vehicle (n = 8) and linifanib (n = 10) treated groups in the U87MG model. There was a significant decrease in tumor volume with linifanib therapy compared to vehicle treatment beginning at day 4 ($p < 0.05$). The %ID tumor uptake of ^{99m}Tc-3P-RGD$_2$ peaked in the vehicle-treated group (n = 8) at day 11 (Figure 2A), while the %ID/cm^3 tumor uptake decreased slowly over the whole study period (Figure 2B). In the linifanib-treated group (n = 10), there was a significant reduction in both %ID/cm^3 and tumor/muscle ratio (T/M) of ^{99m}Tc-3P-RGD$_2$ compared to vehicle as early as 24 h after linifanib treatment ($p < 0.05$) and remained decreased compared to vehicle at subsequent time points until day 18. The difference between linifanib and vehicle treated groups was not significant until day 4 with %ID (Figure 2A). The reduction in ^{99m}Tc-3P-RGD$_2$ tumor uptake observed with linifanib treatment is further illustrated by SPECT/CT images in Figure 3.

Linifanib Therapy in the PC-3 Tumor Model. As shown in Figure 1B, there was no significant difference in tumor volumes between vehicle (n = 8) and linifanib-treated (n = 8) groups. No significant difference in ^{99m}Tc-3P-RGD$_2$ tumor uptake was observed between these two groups by %ID (Figure 2D), %ID/cm^3 (Figure 2E), or T/M ratio (Figure 2F) at any of the five imaging time points.

Effects of Linifanib Treatment on $\alpha_v\beta_3$ Expression. Figure 4 shows images of histological tumor slices from both U87MG (upper panel) and PC-3 (lower panel) models.

JPET Fast Forward. Published on June 7, 2013 as DOI: 10.1124/jpet.112.202622
This article has not been copyedited and formatted. The final version may differ from this version.

U87MG tumors exhibited a high density of blood vessels while the PC-3 tumors had a low density of blood vessels prior to linifanib therapy as indicated by the high integrin β_3 and CD31 expression on U87MG tumors and low expression of β_3 and CD31 on PC-3 tumors prior to starting treatment (Figure 5). After linifanib therapy, both β_3 and CD31 expression in the U87MG tumors diminished while there was little change in the PC-3 tumors (Figure 5).

Immunohistochemical staining was performed to explore the expression patterns of CD31 and $\alpha_v\beta_3$ in the U87MG and PC-3 tumors during treatment and to understand the differences in tumor uptake of ^{99m}Tc-3P-RGD$_2$. Figure 5 shows overlay images of U87MG tumors harvested at -1, 1, 4, 11 and 18 days after initiation of linifanib therapy. Within the first 24 h after the initiation of linifanib therapy, the main effect was on tumor neovasculature as indicated by the disappearance of β_3 on tumor vasculature. By day 4, β_3 on tumor vasculature disappeared completely while the intensity of β_3 on tumor cells decreased steadily (Figure 5). By day 18, there was extensive necrosis in tumors from both vehicle and linifanib treated groups. Very little CD31 and β_3 expression was detected in necrotic regions while CD31 and β_3 were highly expressed in the viable region.

Maximal Decrease in $\alpha_v\beta_3$ Expression and Minimal Time to Achieve Maximal Decrease in $\alpha_v\beta_3$ Expression. A slow reduction ($p < 0.05$) compared to baseline in both tumor uptake and T/M ratio of ^{99m}Tc-3P-RGD$_2$ in the vehicle group (Figure 6) was observed during the first 4 days. The tumor response curve for the vehicle-treated group was modeled by a linear regression with R^2 being 0.921 for the %ID/cm^3 tumor uptake and 0.976 for T/M ratios. During the first 4 days after initiation of linifanib therapy, there was a very fast decrease compared to baseline in both the %ID/cm^3 tumor uptake (Figure 6A) and T/M ratios (Figure 6B) of ^{99m}Tc-3P-RGD$_2$ followed by a slow decrease over the next 14 days ($p < 0.05$). The cross-point of the two phases indicates the maximal decrease in $\alpha_v\beta_3$ expression and minimal time to achieve the maximum decrease in $\alpha_v\beta_3$ expression for this dose of linifanib in the U87MG model. The tumor

JPET Fast Forward. Published on June 7, 2013 as DOI: 10.1124/jpet.112.202622
This article has not been copyedited and formatted. The final version may differ from this version.

response curve was modeled by an exponential decay with R^2 being 0.985 for the %ID/cm^3 tumor uptake and 0.932 for T/M ratio. The maximal tumor decrease in $\alpha_v\beta_3$ expression was calculated to be 70 ± 7% from the %ID/cm^3 tumor uptake plot and 66 ± 14% from T/M ratio plot. The calculated time to achieve maximal decrease in $\alpha_v\beta_3$ expression was 1.65 days for the %ID/cm^3 tumor uptake plot and 1.52 days for T/M ratio plot (Figure 6).

JPET Fast Forward. Published on June 7, 2013 as DOI: 10.1124/jpet.112.202622
This article has not been copyedited and formatted. The final version may differ from this version.

DISCUSSION

Because growth factors, including VEGF, increase the expression of $\alpha_v\beta_3$ (Distler et al., 2003), inhibition of VEGF and PDGF receptors could lead to decreased $\alpha_v\beta_3$ expression. This makes $\alpha_v\beta_3$ a mechanistically relevant biomarker for assessing downstream biological effects of linfanib therapy, which specifically targets VEGF and PDGF receptors. Vascular changes in response to linifanib have been previously been demonstrated by DCE-MRI preclinically and clinically, but changes in $\alpha_v\beta_3$ expression have not been reported (Wong et al., 2009; Jiang et al., 2011; Tannir et al., 2011; Luo et al., 2012). In this study, decreases in the tumor uptake (%ID/cm^3 and T/M ratio) of ^{99m}Tc-3P-RGD$_2$ were observed prior to tumor volume changes in the U87MG model after linifanib treatment (Figures 2). No significant changes in tumor uptake of ^{99m}Tc-3P-RGD$_2$ or corresponding tumor volume changes were seen in the PC-3 model (Figures 1 and 2), indicating a lack of efficacy of linifanib therapy in this animal model. The changes in tumor vasculature were confirmed by histopathological H&E analysis (Figure 4) after the last SPECT/CT imaging time point and further support the use of ^{99m}Tc-3P-RGD$_2$ - SPECT as a biomarker for linifanib. The time to achieve maximal decrease in $\alpha_v\beta_3$ (Figure 6) expression could be used to provide an indication of early PD response as well as guide design of biomarker aspects of clinical studies.

The efficacy observed with linifanib therapy in the U87MG model (high $\alpha_v\beta_3$ and CD31 expression) but not in the PC-3 model (low $\alpha_v\beta_3$ and CD31 expression) is consistent with the parallel relationship between $\alpha_v\beta_3$ and VEGFR2. Highly vascularized tumors have a higher expression level of $\alpha_v\beta_3$ and VEGFR2 than poorly vascularized tumors (Provias et al., 1997; Perrone et al., 2004; Tsutsui et al., 2005; Li et al., 2008). However, the predictive value of treatment outcome with initial VEGFR expression has had mixed results (Jain et al., 2009). Nevertheless, $\alpha_v\beta_3$ expression level should be explored as a patient selection biomarker. Due to the limited number of animal models used in the present study, additional studies in models

with intermediate levels of $\alpha_v\beta_3$ expression are warranted to further investigate if ^{99m}Tc-3P-RGD$_2$ SPECT/CT is useful as a non-invasive biomarker for patient selection.

Linifanib targets multiple tyrosine kinases; of which, VEGFR2 and PDGFR directly interact with $\alpha_v\beta_3$. Inhibiting VEGFR2 and PDGFR may cause endothelial cells to undergo apoptosis, which would directly decrease the number of $\alpha_v\beta_3$ expressing cells. Flt1 and CSF-1 (members of the VEGF and PDGF receptor families, respectively), which are inhibited by linifanib (Albert et al., 2006), regulate the production and activiation of macrophages that accelerate the breakdown of the ECM. Breakdown of the ECM can cause exposure of sites recognized by $\alpha_v\beta_3$ and can likely allow newly sprouting vessels to interact with the remodeled ECM (Weis and Cheresh, 2011), which may also influence tracer uptake. Decreasing the leakiness of the vasculature by inhibiting VEGFR may also lead to a decrease in tumor uptake of ^{99m}Tc-3P-RGD$_2$, by limiting the amount available for both specific and non-specific binding. However, the decrease in $\alpha_v\beta_3$ expression observed post-treatment with linifanib by IHC indicates this scenario is less likely.

The contribution from tumor cells and vasculature on the uptake of ^{99m}Tc-3P-RGD$_2$ is unknown. Because of limitations in spatial resolution, it cannot be directly determined if changes in $\alpha_v\beta_3$ expression are due to changes on neovasculature, tumor cells, or both. It was reported that linifanib was able to normalize >75% of tumor vasculature by day 4, as evidenced by the disappearance of leaky microvessels (Jiang et al., 2011). If linifanib therapy had minimal impact on tumor cells compared to vasculature at day 4, it can be estimated that the % contribution from neovasculature to the $\alpha_v\beta_3$ expression and tumor uptake of ^{99m}Tc-3P-RGD$_2$ is ~60% in the U87MG model. This estimation is supported by the fact that the tumor uptake of ^{99m}Tc-3P-RGD$_2$ (Figure 2) at day 4 was ~40% of its value at -1 day.

^{18}F-labeled RGD peptides, such as ^{18}F-Fluciclatide and ^{18}F-FPPRGD2 have been used as PET radiotracers to monitor tumor response to antiangiogenic therapy with sunitinib,

JPET Fast Forward. Published on June 7, 2013 as DOI: 10.1124/jpet.112.202622
This article has not been copyedited and formatted. The final version may differ from this version.

ZD4190, and paclitaxel preclinically (Morrison et al., 2009; Battle et al., 2011; Sun et al., 2011). Results from this study agree with previously published reports providing evidence for imaging the $\alpha_v\beta_3$ in response to therapy. However, imaging integrin expression has yet to be utilized to monitor treatment response clinically. Considering the kinetics, biodistribution, radiation dosimetry and clinical availability, we believe that ^{99m}Tc-3P-RGD$_2$ has significant advantages over the ^{18}F-labeled cyclic RGD peptide radiotracers. The linear relationship between T/M ratios of ^{99m}Tc-3P-RGD$_2$ and expression levels of $\alpha_v\beta_3$ and CD31 (Zhou et al., 2011; Zhou et al., 2012a) could potentially make semi-quantitative SPECT imaging of ^{99m}Tc-3P-RGD$_2$ more practical clinically. Therefore, further investigations are warranted to better understand how changes in tumor uptake and T/M ratios of ^{99m}Tc-3PRGD reflect the tumor response to antiangiogenic treatment before it can be used clinically to monitor investigational therapy.

JPET Fast Forward. Published on June 7, 2013 as DOI: 10.1124/jpet.112.202622
This article has not been copyedited and formatted. The final version may differ from this version.

CONCLUSION

An early decrease in tumor ^{99m}Tc-3P-RGD$_2$ uptake, which corresponded to efficacy, was observed with linifanib therapy in the U87MG xenograft glioma model, but not in the PC-3 xenograft model of prostate cancer. Vascular changes in response to linifanib treatment were confirmed by H&E analysis and IHC. SPECT/CT imaging with ^{99m}Tc-3P-RGD$_2$ is a promising method for noninvasive monitoring of early downstream biological response to linifanib therapy. Additional studies in tumor models with intermediate levels of $\alpha_v\beta_3$ expression are warranted to further verify ^{99m}Tc-3P-RGD$_2$ SPECT/CT as a screening tool for patient selection and to better understand how changes in tumor uptake reflect tumor response to antiangiogenic treatment before ^{99m}Tc-3P-RGD$_2$ can be used clinically to monitor investigational therapy.

ACKNOWLEDGMENTS

The authors wish to thank Dr. Aaron B. Taylor for technical assistance with SPECT/CT studies at the Purdue University Imaging Center. The authors also wish to thank Todd Cole and Paul Tapang of Abbvie, Inc. for their contributions in enabling this study.

AUTHORSHIP CONTRIBUTIONS

Participated in research design: Zhang, Fox, Albert, Luo, Liu, Mudd

Conducted experiments: Ji, Zhou, and Shao

Performed data analysis: Ji, Zhou, Voorbach, Liu, Mudd

Wrote or contributed to the writing, review, and approval of the manuscript: Albert, Fox, Ji, Liu, Luo, Mudd, Shao, Voorbach, Zhang, Zhou

REFERENCES

Albert DH, Tapang P, Magoc TJ, Pease LJ, Reuter DR, Wei RQ, Li J, Guo J, Bousquet PF, Ghoreishi-Haack NS, Wang B, Bukofzer GT, Wang YC, Stavropoulos JA, Hartandi K, Niquette AL, Soni N, Johnson EF, McCall JO, Bouska JJ, Luo Y, Donawho CK, Dai Y, Marcotte PA, Glaser KB, Michaelides MR and Davidsen SK (2006) Preclinical activity of ABT-869, a multitargeted receptor tyrosine kinase inhibitor. *Mol Cancer Ther* **5**:995-1006.

Battle MR, Goggi JL, Allen L, Barnett J and Morrison MS (2011) Monitoring tumor response to antiangiogenic sunitinib therapy with 18F-fluciclatide, an ^{18}F-labeled $\alpha_V\beta_3$-integrin and $\alpha_V\beta_5$-integrin imaging agent. *J Nucl Med* **52**:424-430.

Bergers G and Benjamin LE (2003) Tumorigenesis and the angiogenic switch. *Nat Rev Cancer* **3**:401-410.

Bergers G, Song S, Meyer-Morse N, Bergsland E and Hanahan D (2003) Benefits of targeting both pericytes and endothelial cells in the tumor vasculature with kinase inhibitors. *J Clin Invest* **111**:1287-1295.

Borges E, Jan Y and Ruoslahti E (2000) Platelet-derived growth factor receptor beta and vascular endothelial growth factor receptor 2 bind to the β_3 integrin through its extracellular domain. *J Biol Chem* **275**:39867-39873.

Cao Y, Arbiser J, D'Amato RJ, D'Amore PA, Ingber DE, Kerbel R, Klagsbrun M, Lim S, Moses MA, Zetter B, Dvorak H and Langer R (2011) Forty-year journey of angiogenesis translational research. *Sci Transl Med* **3**:114rv113.

Chakraborty S, Shi J, Kim YS, Zhou Y, Jia B, Wang F and Liu S (2010) Evaluation of ^{111}In-labeled cyclic RGD peptides: tetrameric not tetravalent. *Bioconjug Chem* **21**:969-978.

Clemmons DR, Horvitz G, Engleman W, Nichols T, Moralez A and Nickols GA (1999) Synthetic $\alpha_V\beta_3$ antagonists inhibit insulin-like growth factor-I-stimulated smooth muscle cell migration and replication. *Endocrinology* **140**:4616-4621.

Cybulsky AV, McTavish AJ and Cyr MD (1994) Extracellular matrix modulates epidermal growth factor receptor activation in rat glomerular epithelial cells. *J Clin Invest* **94**:68-78.

Desgrosellier JS and Cheresh DA (2010) Integrins in cancer: biological implications and therapeutic opportunities. *Nat Rev Cancer* **10**:9-22.

Distler JH, Hirth A, Kurowska-Stolarska M, Gay RE, Gay S and Distler O (2003) Angiogenic and angiostatic factors in the molecular control of angiogenesis. *Q J Nucl Med* **47**:149-161.

Dunn IF, Heese O and Black PM (2000) Growth factors in glioma angiogenesis: FGFs, PDGF, EGF, and TGFs. *J Neurooncol* **50**:121-137.

Ferrara N and Kerbel RS (2005) Angiogenesis as a therapeutic target. *Nature* **438**:967-974.

Heldin CH, Ostman A and Ronnstrand L (1998) Signal transduction via platelet-derived growth factor receptors. *Biochim Biophys Acta* **1378**:F79-113.

Hernandez-Davies JE, Zape JP, Landaw EM, Tan X, Presnell A, Griffith D, Heinrich MC, Glaser KB and Sakamoto KM (2011) The multitargeted receptor tyrosine kinase inhibitor linifanib (ABT-869) induces apoptosis through an Akt and glycogen synthase kinase 3β-dependent pathway. *Mol Cancer Ther* **10**:949-959.

Jain RK, Duda DG, Willett CG, Sahani DV, Zhu AX, Loeffler JS, Batchelor TT and Sorensen AG (2009) Biomarkers of response and resistance to antiangiogenic therapy. *Nat Rev Clin Oncol* **6**:327-338.

Jeswani T and Padhani AR (2005) Imaging tumour angiogenesis. *Cancer Imaging* **5**:131-138.

Jia B, Liu Z, Zhu Z, Shi J, Jin X, Zhao H, Li F, Liu S and Wang F (2011) Blood clearance kinetics, biodistribution, and radiation dosimetry of a kit-formulated integrin $\alpha_v\beta_3$-selective radiotracer ^{99m}Tc-3PRGD$_2$ in non-human primates. *Mol Imaging Biol* **13**:730-736.

Jiang F, Albert DH, Luo Y, Tapang P, Zhang K, Davidsen SK, Fox GB, Lesniewski R and McKeegan EM (2011) ABT-869, a multitargeted receptor tyrosine kinase inhibitor, reduces tumor microvascularity and improves vascular wall integrity in preclinical tumor models. *J Pharmacol Exp Ther* **338**:134-142.

Jones PL, Crack J and Rabinovitch M (1997) Regulation of tenascin-C, a vascular smooth muscle cell survival factor that interacts with the $\alpha_v\beta_3$ integrin to promote epidermal growth factor receptor phosphorylation and growth. *J Cell Biol* **139**:279-293.

Li SG, Ye ZY, Zhao ZS, Tao HQ, Wang YY and Niu CY (2008) Correlation of integrin β_3 mRNA and vascular endothelial growth factor protein expression profiles with the clinicopathological features and prognosis of gastric carcinoma. *World J Gastroenterol* **14**:421-427.

Luo Y, Jiang F, Cole TB, Hradil VP, Reuter D, Chakravartty A, Albert DH, Davidsen SK, Cox BF, McKeegan EM and Fox GB (2012) A novel multi-targeted tyrosine kinase inhibitor, linifanib (ABT-869), produces functional and structural changes in tumor vasculature in an orthotopic rat glioma model. *Cancer Chemother Pharmacol* **69**:911-921.

Ma Q, Ji B, Jia B, Gao S, Ji T, Wang X, Han Z and Zhao G (2011) Differential diagnosis of solitary pulmonary nodules using ^{99m}Tc-3P$_4$-RGD$_2$ scintigraphy. *Eur J Nucl Med Mol Imaging* **38**:2145-2152.

Mahabeleshwar GH, Feng W, Reddy K, Plow EF and Byzova TV (2007) Mechanisms of integrin-vascular endothelial growth factor receptor cross-activation in angiogenesis. *Circ Res* **101**:570-580.

Morrison MS, Ricketts SA, Barnett J, Cuthbertson A, Tessier J and Wedge SR (2009) Use of a novel Arg-Gly-Asp radioligand, ^{18}F-AH111585, to determine changes in tumor vascularity after antitumor therapy. *J Nucl Med* **50**:116-122.

O'Connor JP, Jackson A, Parker GJ and Jayson GC (2007) DCE-MRI biomarkers in the clinical evaluation of antiangiogenic and vascular disrupting agents. *Br J Cancer* **96**:189-195.

Perrone G, Vincenzi B, Santini D, Verzi A, Tonini G, Vetrani A and Rabitti C (2004) Correlation of p53 and bcl-2 expression with vascular endothelial growth factor (VEGF), microvessel density (MVD) and clinico-pathological features in colon cancer. *Cancer Lett* **208**:227-234.

Provias J, Claffey K, delAguila L, Lau N, Feldkamp M and Guha A (1997) Meningiomas: role of vascular endothelial growth factor/vascular permeability factor in angiogenesis and peritumoral edema. *Neurosurgery* **40**:1016-1026.

Shankar DB, Li J, Tapang P, Owen McCall J, Pease LJ, Dai Y, Wei RQ, Albert DH, Bouska JJ, Osterling DJ, Guo J, Marcotte PA, Johnson EF, Soni N, Hartandi K, Michaelides MR, Davidsen SK, Priceman SJ, Chang JC, Rhodes K, Shah N, Moore TB, Sakamoto KM and Glaser KB (2007) ABT-869, a multitargeted receptor tyrosine kinase inhibitor: inhibition of FLT3 phosphorylation and signaling in acute myeloid leukemia. *Blood* **109**:3400-3408.

Shao G, Zhou Y, Wang F and Liu S (2013) Monitoring Glioma Growth and Tumor Necrosis with the U-SPECT-II/CT Scanner by Targeting Integrin alphavbeta3. *Mol Imaging* **12**:39-48.

Shattil SJ (1995) Function and regulation of the beta 3 integrins in hemostasis and vascular biology. *Thromb Haemost* **74**:149-155.

Shi J, Kim YS, Chakraborty S, Jia B, Wang F and Liu S (2009a) 2-Mercaptoacetylglycylglycyl (MAG2) as a bifunctional chelator for ^{99m}Tc-labeling of cyclic RGD dimers: effect of technetium chelate on tumor uptake and pharmacokinetics. *Bioconjug Chem* **20**:1559-1568.

Shi J, Wang L, Kim YS, Zhai S, Jia B, Wang F and Liu S (2009b) ^{99m}TcO(MAG2-3G3-dimer): a new integrin $\alpha_v\beta_3$-targeted SPECT radiotracer with high tumor uptake and favorable pharmacokinetics. *Eur J Nucl Med Mol Imaging* **36**:1874-1884.

Shi J, Zhou Y, Chakraborty S, Kim YS, Jia B, Wang F and Liu S (2011) Evaluation of In-Labeled Cyclic RGD Peptides: Effects of Peptide and Linker Multiplicity on Their Tumor Uptake, Excretion Kinetics and Metabolic Stability. *Theranostics* **1**:322-340.

Soldi R, Mitola S, Strasly M, Defilippi P, Tarone G and Bussolino F (1999) Role of $\alpha_v\beta_3$ integrin in the activation of vascular endothelial growth factor receptor-2. *EMBO J* **18**:882-892.

Somanath PR, Ciocea A and Byzova TV (2009) Integrin and growth factor receptor alliance in angiogenesis. *Cell Biochem Biophys* **53**:53-64.

Sun X, Yan Y, Liu S, Cao Q, Yang M, Neamati N, Shen B, Niu G and Chen X (2011) ^{18}F-FPPRGD2 and ^{18}F-FDG PET of response to Abraxane therapy. *J Nucl Med* **52**:140-146.

Tannir NM, Wong YN, Kollmannsberger CK, Ernstoff MS, Perry DJ, Appleman LJ, Posadas EM, Cho D, Choueiri TK, Coates A, Gupta N, Pradhan R, Qian J, Chen J, Scappaticci FA, Ricker JL, Carlson DM and Michaelson MD (2011) Phase 2 trial of linifanib (ABT-869) in patients with advanced renal cell cancer after sunitinib failure. *Eur J Cancer* **47**:2706-2714.

Tsutsui S, Yasuda K, Suzuki K, Tahara K, Higashi H and Era S (2005) Macrophage infiltration and its prognostic implications in breast cancer: the relationship with VEGF expression and microvessel density. *Oncol Rep* **14**:425-431.

Wang L, Shi J, Kim YS, Zhai S, Jia B, Zhao H, Liu Z, Wang F, Chen X and Liu S (2009) Improving tumor-targeting capability and pharmacokinetics of ^{99m}Tc-labeled cyclic RGD dimers with PEG_4 linkers. *Mol Pharm* **6**:231-245.

Weis SM and Cheresh DA (2011) Tumor angiogenesis: molecular pathways and therapeutic targets. *Nat Med* **17**:1359-1370.

Wong CI, Koh TS, Soo R, Hartono S, Thng CH, McKeegan E, Yong WP, Chen CS, Lee SC, Wong J, Lim R, Sukri N, Lim SE, Ong AB, Steinberg J, Gupta N, Pradhan R, Humerickhouse R and Goh BC (2009) Phase I and biomarker study of ABT-869, a multiple receptor tyrosine kinase inhibitor, in patients with refractory solid malignancies. *J Clin Oncol* **27**:4718-4726.

Woodard AS, Garcia-Cardena G, Leong M, Madri JA, Sessa WC and Languino LR (1998) The synergistic activity of alphavbeta3 integrin and PDGF receptor increases cell migration. *J Cell Sci* **111 (Pt 4)**:469-478.

Zhou J, Goh BC, Albert DH and Chen CS (2009) ABT-869, a promising multi-targeted tyrosine kinase inhibitor: from bench to bedside. *J Hematol Oncol* **2**:33.

Zhou Y, Kim YS, Chakraborty S, Shi J, Gao H and Liu S (2011) ^{99m}Tc-labeled cyclic RGD peptides for noninvasive monitoring of tumor integrin $\alpha_V\beta_3$ expression. *Mol Imaging* **10**:386-397.

Zhou Y, Kim YS, Lu X and Liu S (2012a) Evaluation of ^{99m}Tc-labeled cyclic RGD dimers: impact of cyclic RGD peptides and ^{99m}Tc chelates on biological properties. *Bioconjug Chem* **23**:586-595.

Zhou Y, Shao G and Liu S (2012b) Monitoring Breast Tumor Lung Metastasis by U-SPECT-II/CT with an Integrin $\alpha_v\beta_3$-Targeted Radiotracer ^{99m}Tc-3P-RGD$_2$. *Theranostics* **2**:577-588.

Zhu Z, Miao W, Li Q, Dai H, Ma Q, Wang F, Yang A, Jia B, Jing X, Liu S, Shi J, Liu Z, Zhao Z and Li F (2012) ^{99m}Tc-3PRGD$_2$ for integrin receptor imaging of lung cancer: a multicenter study. *J Nucl Med* **53**:716-722.

Footnotes

This work was supported in part by Purdue University. Research grants supported Yang Zhou and Shuang Liu at Purdue: from the National Cancer Institute [R01 CA115883] and from the Susan G. Komen Breast Cancer Foundation [KG111333].

This work was funded in part by AbbVie Inc. AbbVie Inc. and Purdue University contributed to the study design, interpretation of data, writing, review, and approving the publication. Martin Voorbach, Yumin Zhang, Gerard Fox, Daniel Albert, Yanping Luo, and Sarah Mudd are employees of AbbVie Inc.

Legends for Figures

Figure 1. Comparison of tumor volumes in vehicle (n = 8 for both U87MG and PC-3) and linifanib-treated (n = 10 for U87MG and n = 8 for PC-3) groups in the U87MG (A) and PC-3 (B) models. Tumor volumes were determined by caliper measurements.

Figure 2. Comparison of the %ID tumor uptake (**A** and **D**), %ID/cm^3 tumor uptake (**B** and **E**), and tumor/muscle ratios (**C** and **F**) of ^{99m}Tc-3P-RGD_2 in vehicle (n = 8 for both U87MG and PC-3) and linifanib-treated (n = 10 for U87MG and n = 8 for PC-3) groups. Tumor uptake values and T/M ratios were calculated from quantification of SPECT/CT images obtained for U87MG (left) and PC-3 (right) models. Significance is indicated by *.

Figure 3. Transverse views of selected SPECT/CT images from athymic nude mice bearing U87MG glioma (top) and PC-3 prostate cancer (bottom) tumors in the vehicle (upper panel) and linifanib-treated groups (lower panel). SPECT/CT images were obtained at baseline (-1), 1, 4, 11 and 18 days after initiation of linifanib therapy. Tumors at baseline are indicated by arrows.

Figure 4. Images of selected histological slice (H&E stained) of tumor tissues (U87MG vs. PC-3) from animals before treatment (left) and after 18 days of linifanib treatment (right) groups to illustrate vascular density changes after linifanib therapy.

Figure 5. Overlay images of U87MG (top) and PC-3 (bottom) tumor tissues after immunohistochemical staining for integrin β_3 and CD31 in vehicle and linifanib-treated groups to illustrate the changes in integrin β_3 expression level and blood vessel density during therapy. Tumor tissues were harvested at -1, 1, 4, 11 and 18 days after initiation of linifanib therapy. CD31 was used as the marker for tumor blood vessels (both mature and newly formed), which was visualized with FITC (green color). Integrin β_3 was visualized with Cy3 (red color). The yellow color in overlay images indicates the integrin β_3 expression on new blood vessels. Magnification was ×200 in all images.

JPET Fast Forward. Published on June 7, 2013 as DOI: 10.1124/jpet.112.202622

Figure 6. Biological response evaluated by tumor time activity curves for %ID/cm^3 (**top**) and T/M ratios (**bottom**) of ^{99m}Tc-3P-RGD$_2$ uptake in the vehicle (n = 8) and linifanib (n = 10) treated groups in the U87MG tumor model. Tumor %ID/cm^3 values and T/M ratios were calculated based on SPECT/CT quantification. Curves were fitted using a linear regression model for the vehicle-treated group and a two-phase exponential decay model (nonlinear regression) for the linifanib-treated group.

JPET Fast Forward. Published on June 7, 2013 as DOI: 10.1124/jpet.112.202622
This article has not been copyedited and formatted. The final version may differ from this version.

Figure 1

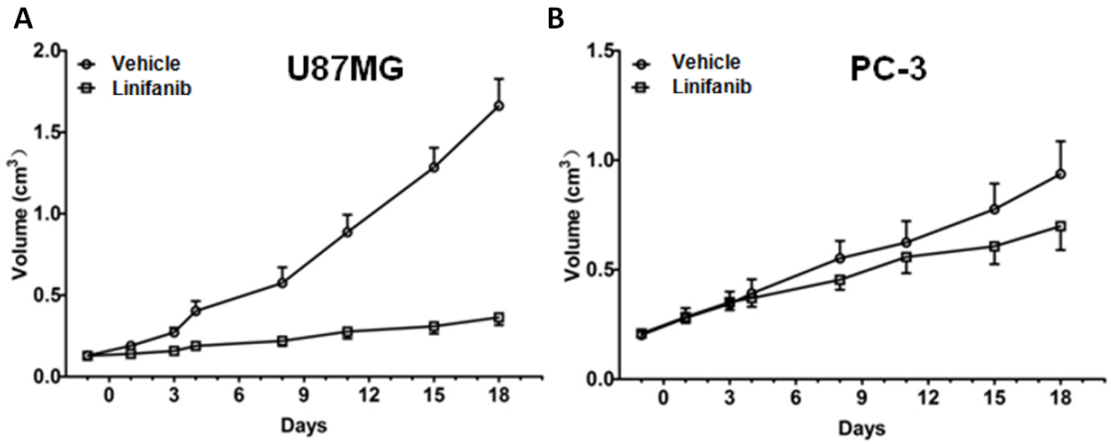

JPET Fast Forward. Published on June 7, 2013 as DOI: 10.1124/jpet.112.202622
This article has not been copyedited and formatted. The final version may differ from this version.

Figure 2

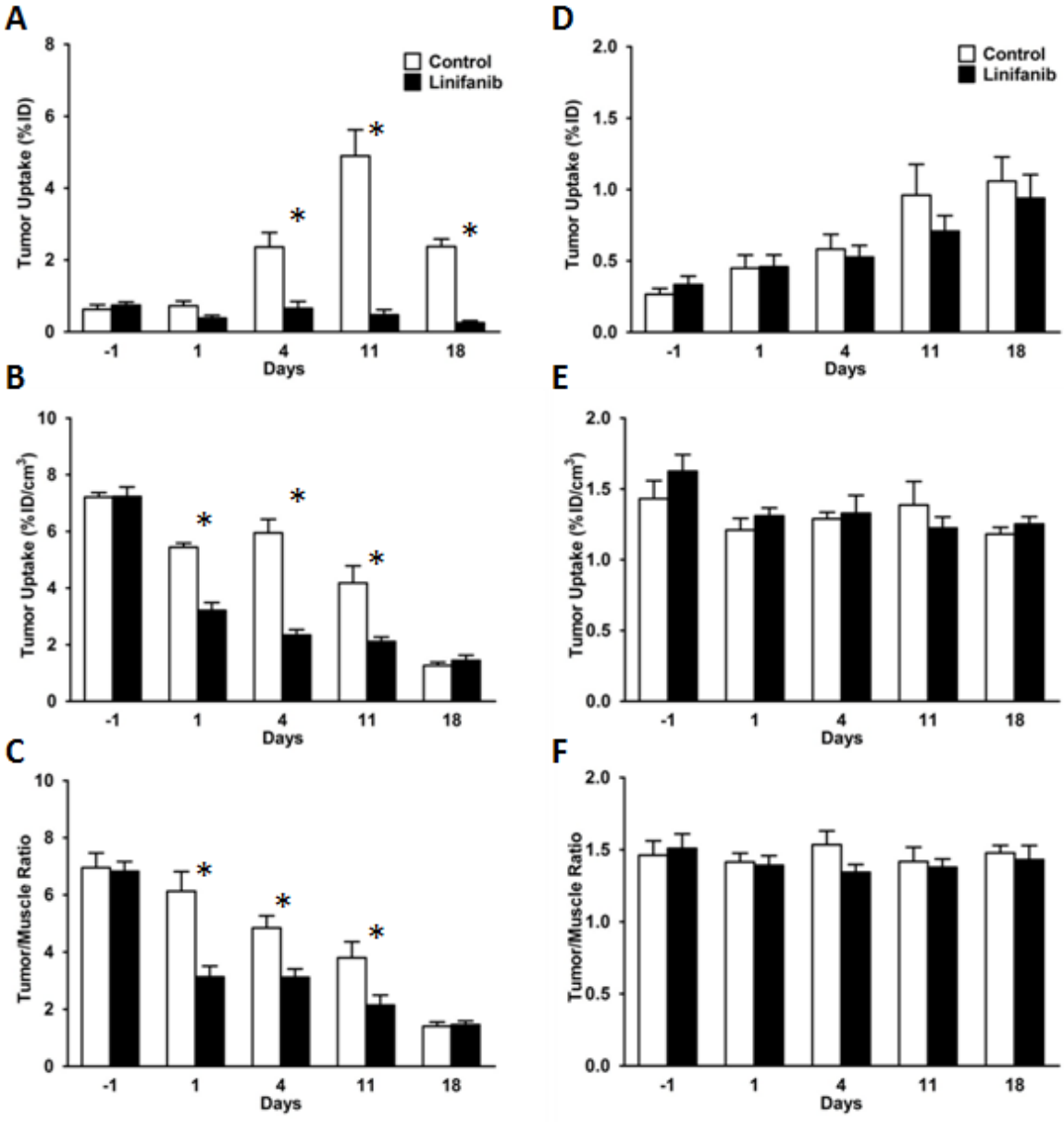

JPET Fast Forward. Published on June 7, 2013 as DOI: 10.1124/jpet.112.202622
This article has not been copyedited and formatted. The final version may differ from this version.

Figure 3

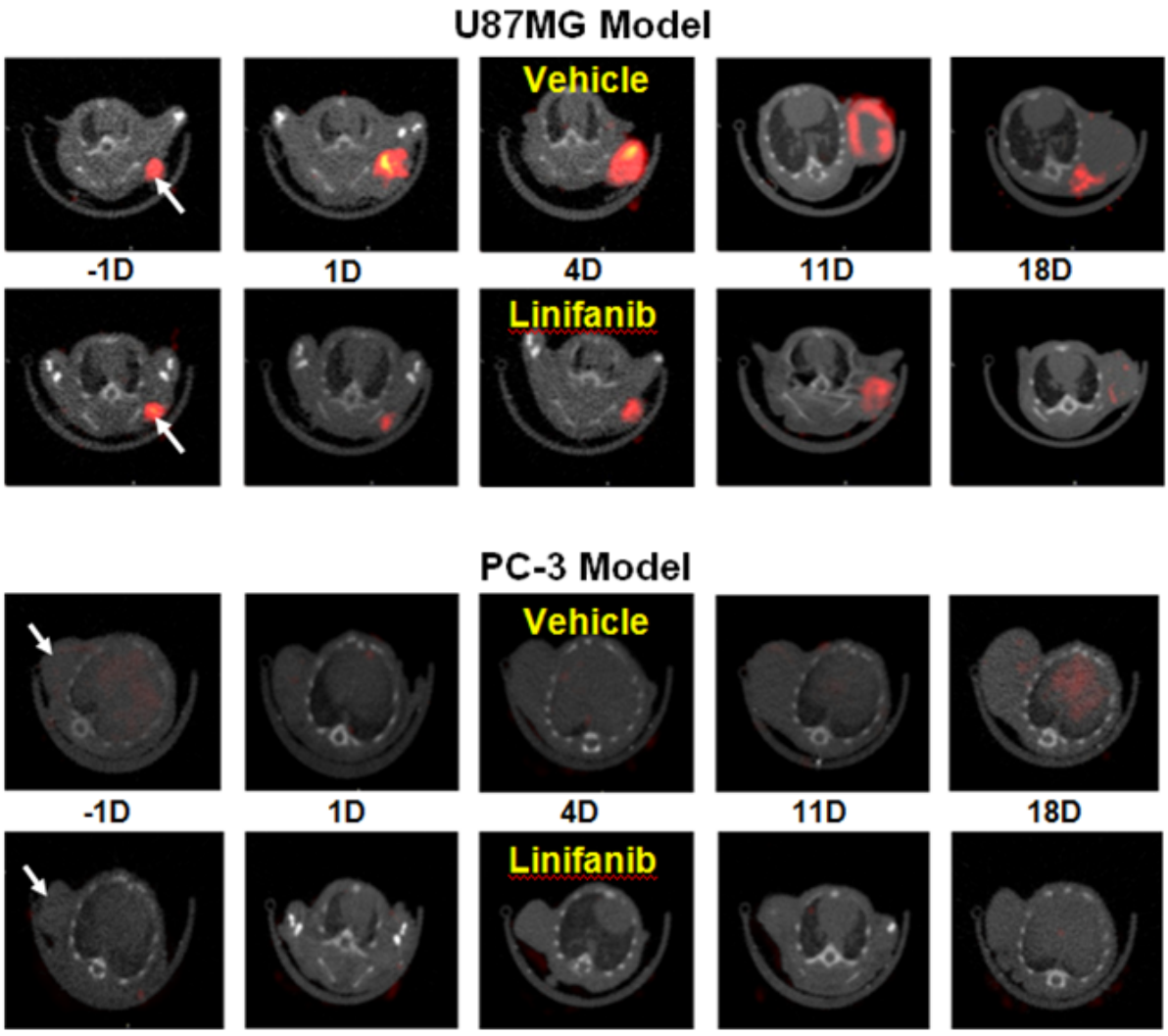

JPET Fast Forward. Published on June 7, 2013 as DOI: 10.1124/jpet.112.202622
This article has not been copyedited and formatted. The final version may differ from this version.

Figure 4

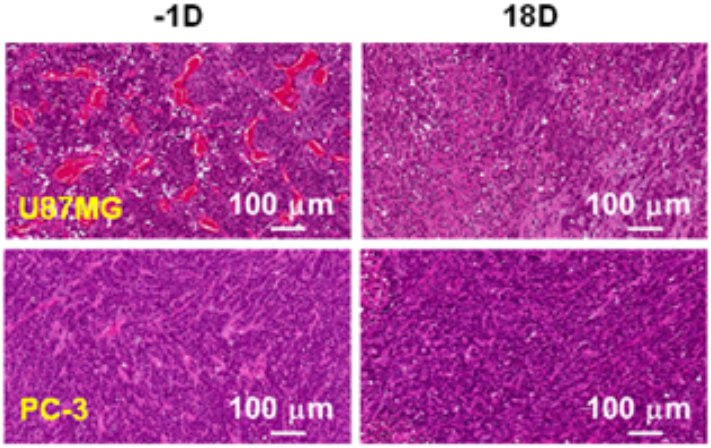

JPET Fast Forward. Published on June 7, 2013 as DOI: 10.1124/jpet.112.202622
This article has not been copyedited and formatted. The final version may differ from this version.

Figure 5

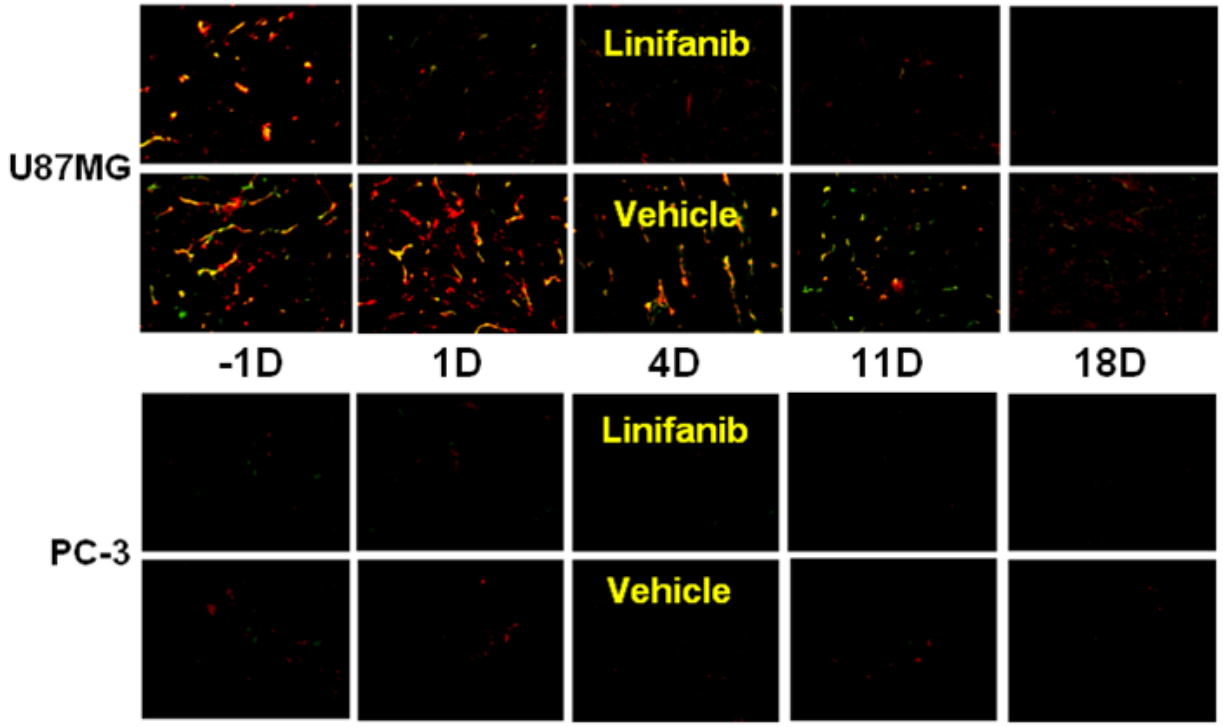

JPET Fast Forward. Published on June 7, 2013 as DOI: 10.1124/jpet.112.202622
This article has not been copyedited and formatted. The final version may differ from this version.

Figure 6